Proceedings of the 11th World Congress on Mechanical, Chemical, and Material Engineering (MCM'25)

Barcelona, Spain -Paris, France - August, 2025

Paper No. HTFF 252 DOI: 10.11159/htff25.252

Anti-Icing System for a NACA0012 Airfoil: A Case Study

Emir M. Koyuncu, Dr. Salih Özen Ünverdi,

¹Gebze Technical University
Eskisehir, Türkiye
emirkoyuncu2022@gtu.edu.tr; sunverdi@gtu.edu.tr

²Gebze Technical University
Gebze, Türkiye

Abstract –Ice accumulation on airfoils can alter the aerodynamic characteristics, leading to performance degradation. In-flight icing starts when metal surfaces encounter supercooled droplets. These droplets are contained in clouds. When an aircraft flies through them, supercooled droplets (below freezing point) may impinge on external surfaces like wing leading edges, fuselage or engine intakes -more specifically, IGVs or inlet particle separators. Furthermore, these droplets may accumulate and freeze (considering free stream temperature is below or equal to zero degrees Celsius) unless a heat source or alternative anti-icing method such as mechanical shedding or chemical treatment is applied. This study investigates the anti-icing heat requirements of a NACA0012 airfoil profile, specifically for the leading-edge region. The heat requirements are calculated using Messinger's approach. External convective heat transfer and droplet collection efficiency values are obtained from experimental data in the literature. Calculated external heat flux terms are used as input for a 2D thermal solver to determine the internal heat flux required to maintain an ice-free surface. Analyses are conducted for two different free-stream velocities: 44.7 m/s and 89.4 m/s. Results indicate a consistent increase in required internal heat flux with increasing free-stream velocity.

Keywords: Anti-Icing, airfoil heat transfer, aircraft icing, IGV anti-icing

1. Introduction

Several methods have been developed to address icing problems in aircraft and aircraft engines. These methods are classified into two main categories: anti-icing and de-icing. De-icing methods are beyond the scope of this study.

Anti-icing methods: Anti-icing ensures that no ice forms on protected surfaces by maintaining their temperature above 0 °C. This method requires continuous surface heating during flight under icing conditions. It is typically an on/off system, activated during flight by either the pilot or an embedded computer system (e.g., FADEC). This method may employ either electrical heating of the protected areas or heating via engine hot bleed air.

To determine the heating required for anti-icing, external heat flux components (i.e., heat losses) must be calculated. These terms represent the thermal effects of supercooled water droplets (i.e., visible moisture within clouds below the freezing point) on the surface temperature of metal surfaces.

The literature includes numerous icing and anti-icing studies—both experimental and numerical—conducted on various aircraft surfaces such as fuselage, wings, and engine inlets. Linkai Li et al. [1] conducted an extensive experimental investigation on a hot-air-based anti-icing system designed for aircraft engine IGVs. They tested an IGV model with an internal U-shaped hot air pipe in an icing wind tunnel, utilizing an imaging system and thermocouples beneath the surface to quantify ice accumulation and surface temperature variations. Their findings revealed that over 80% of the energy absorbed by the surface was attributed to convective heat transfer over the IGV. The normalized droplet collection efficiency distribution for the NACA0012 airfoil exhibited a consistent bell-shaped curve, which could be accurately approximated using a Gaussian function. Al-Khalil et al. [2] tested a NACA0012 airfoil in an icing wind tunnel to determine collection efficiency data. They found that doubling the free-stream velocity increased the droplet collection efficiency at the leading edge from 0.5 to 0.6. Poinsatte et al. [3] conducted wind tunnel tests on a NACA0012 airfoil profile using heat gauges. By measuring the voltage across heat gauges to maintain a constant surface temperature, they obtained Frössling numbers as a function of the non-dimensional surface distance.

2. Mathematical Modelling Details

Heat flux terms are modeled using Messinger's approach [4]. In his study, the heat flux calculations are categorized into three cases. These are: a surface above the freezing point, a surface below the freezing point, and a surface at the freezing point. Since anti-icing aims to maintain an ice-free surface, the "above freezing point" approach is used in this study. The external heat flux terms are represented as follows:

$$Q_{\mathcal{C}} = H_{\mathcal{C}} A \left(T_{\mathcal{S}} - T_{\infty} \right) \tag{1}$$

$$Q_{W} = R_{W} \mathcal{C}_{p_{water}} (T_{S} - T_{\infty}) \tag{2}$$

$$Q_{W} = R_{W} C_{p_{water}} (T_{S} - T_{\infty})$$

$$Q_{e} = \left(0.622 H_{c} / C_{p_{air}}\right) \left(\frac{P_{v,s} - P_{v,l}}{P_{amb} - P_{v,s}}\right)$$

$$Q_{a} = H_{c} I \left(\frac{V_{inf}^{2}}{2 C_{p}}\right)$$

$$Q_{k} = \rho_{air} \beta V_{inf} \frac{V_{inf}^{2}}{2}$$

$$(5)$$

$$Q_{a=}H_{c}I\left(\frac{V_{inf}^{2}}{2C_{D}}\right)^{amb-1V,SJ} \tag{4}$$

$$Q_k = \rho_{air} \beta V_{inf} \frac{V_{inf}^2}{2} \tag{5}$$

$$Q_{net} = Q_a + Q_b + Q_c + Q_e + Q_w \tag{6}$$

Term (1) represents the convective heat transfer between the airfoil surface and the ambient air. Where the H is heat transfer coefficient, A is heat transfer area, T_s is surface temperature, T_{∞} is free stream temperature. Equation (2) represents heat loss due to droplet warming and is defined as the enthalpy exchange between the impinging water and the metal surface. $R_W = \beta LWCV_n$. R_W denotes the rate of water catch. Where β is collection efficiency and defined as the ratio of actual water collected in the area to the maximum water can be collected (dimensionless). LWC is the liquid water content of the cloud (unit as g/m^3). V_n is the normal velocity of the particles against the surface. Equation (3) accounts for heat loss due to evaporation. It is derived using the Chilton-Colburn analogy from $Q_e = \dot{m}_{evap} LE$ [5]. Here \dot{m}_{evap} is mass transfer by evaporation. LE is latent heat of water vaporization. In (3) C_{pair} is the specific heat of air, $P_{v,s}$ is partial pressure of water vapor at the surface, $P_{v,l}$ is the partial pressure of water vapour in the bulk air, P_{amb} is the ambient pressure. Equation (4) describes heat gain due to viscous heating, which results from aerodynamic friction between the surface and the free-stream airflow. Here r is the recovery factor, V_{inf} is the free stream air velocity. Equation (5) is the heat gained due to kinetic energy transfer from the particles. As the particles impinge the metal surfaces, total kinetic energy of the particles is converted into the heat flux. Here ρ_{air} is the density of air.



Figure 1: Total external heat load represented

2.1. Physical Model Details

In this study a NACA0012 profile with a chord length of 0.914 m is used. Since this geometry is symmetrical, only top half of the geometry was used to simplify the model. Only the leading-edge portion of the blade was used (specifically %9 S/C of the full model). Angle of attack was set to 0°. Ambient temperature set as 263K, pressure 101.325 kPa, LWC defined

as 2.2 g/m^3 . Collection efficiency (β) at the stagnation point calculated using Langmuir et al. [6]. and compared with experimental literature data [2] in the Figure 2 below. Material chosen as A357 (average 160 W/mK of conductivity)

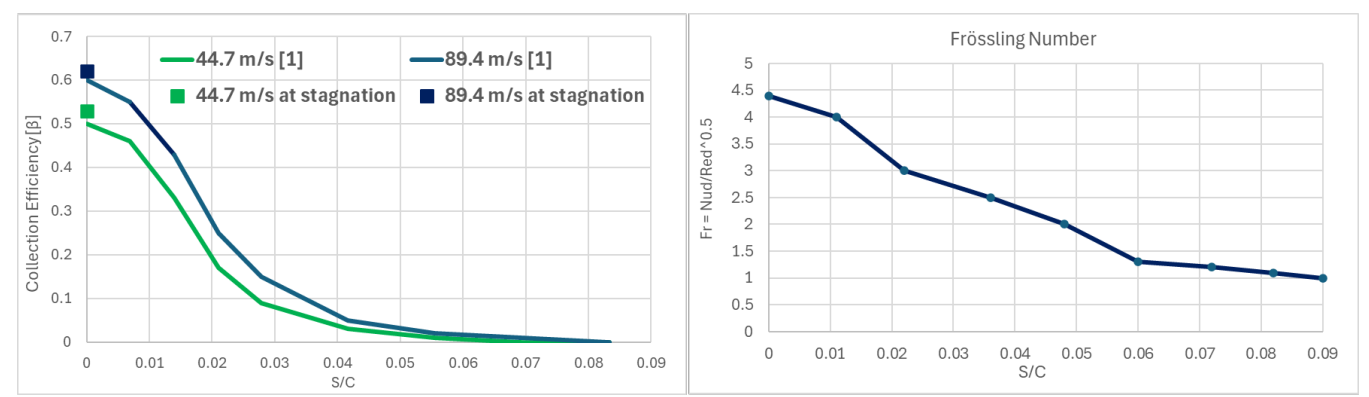


Figure 2: Collection efficiency from literature and hand calculations (on the left), Frössling numbers on the surface (on the right)

From the Figure 2, Frössling number $\left(Fr = \frac{Nu_d}{\sqrt{Re_d}}\right)$ on the surface against S/C values can be seen as experimental data [3]. These Fr numbers are valid for $1.2E6 < Re_d < 4.5E6$, angle of attack 0°.

Finite element model created in the 2D thermal solver. All the equations defined to the surfaces parametrically (changing by S/C). Meshed 2D model can be seen at the Figure 3 below.

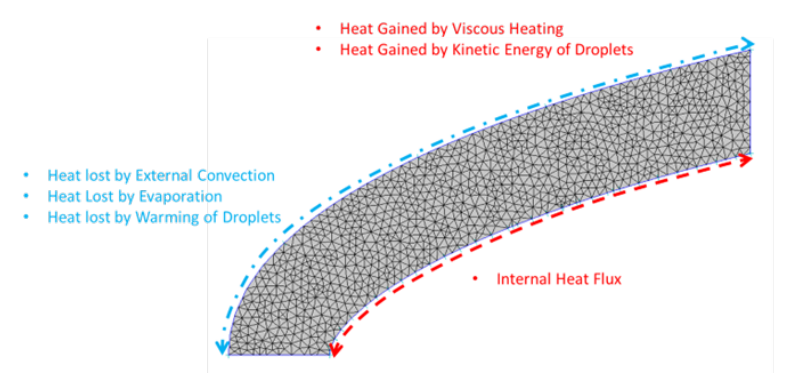


Figure 3: Airfoil finite element model with heat flux terms setup

Analyses solved for 44.7 m/s and 89.7 m/s free stream velocities. Internal heat flux iterated to ensure minimum outer surface temperature kept at minimum 275K.

3. Results

As expected, after targeting a minimum surface temperature of 2 °C, lowest values occur at the leading-edge stagnation point. As the distance from the leading-edge increases, surface temperatures increase. All calculated external heat flux terms are shown in the Figure 4 below. At 44.7 m/s (Case 1) heat gain terms are nearly negligible. As the speed increases to 89.4 m/s, these terms yield a heat flux of almost $2 \, kW/m^2$. From the Table 1, internal heat flux needed (to keep minimum surface temperature at 2 °) is **4.22** kW/m^2 . Case 2 internal heat flux needed is **6.3** kW/m^2 .

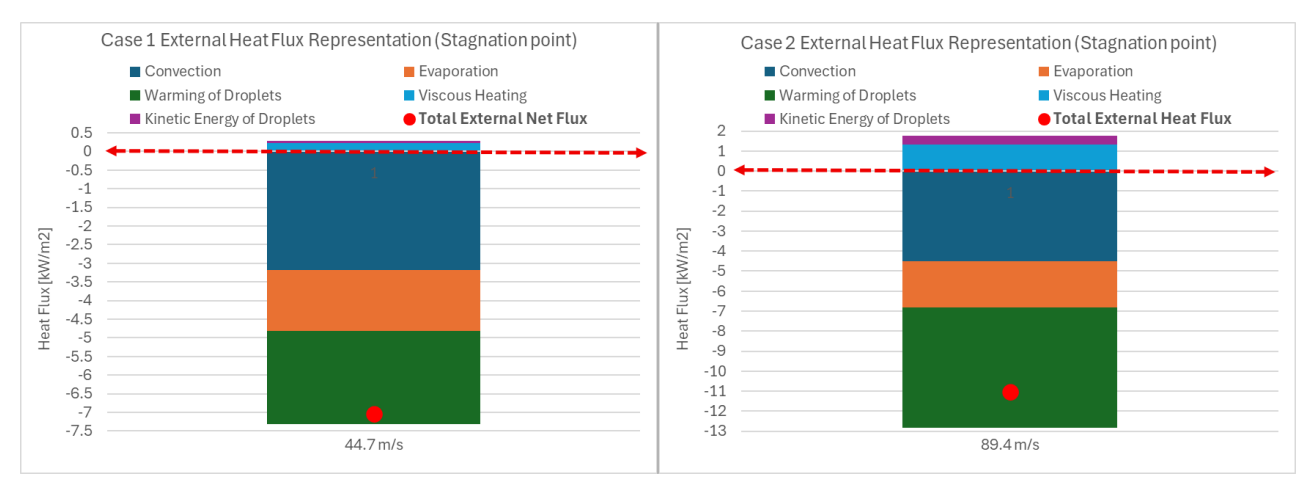


Figure 4: Case1&2 External heat flux terms at the stagnation point

Table 1: Calculated external and internal heat flux terms for both cases

Case 1 (44 7 m/s) Case 2 (89 7 m/s)

	Cusc 1 (++./ 111/3)		Case 2 (07.7 III/3)	
	Surface	Stagnation	Surface	Stagnation
Heat Flux Terms	Average	Point	Average	Point
	[kW/m2]	[kW/m2]	[kW/m2]	[kW/m2]
Convection	-1.78	-3.18	-2.62	-4.51
Evaporation	-0.94	-1.64	-1.42	-2.32
Warming of Droplets	-0.57	-2.49	-1.56	-5.99
Viscous Heating	0.12	0.23	0.69	1.31
Kinetic Energy of Droplets	0.01	0.05	0.12	0.47
Total External Heating	0.13	0.28	0.81	1.78
Total External Cooling	-3.29	-7.31	-5.6	-12.82
Internal Heat Source	4.22		6.3	

4. Conclusions

In conclusion, the calculated internal heat flux requirements indicate that increased free-stream velocities (doubling) demand higher (%50 more) anti-icing energy. These findings provide a useful benchmark for the design of airfoil anti-icing systems utilizing either bleed air or electrical heating methods.

References

- [1] L. Li, Y. Liu "An experimental study on a hot-air-based anti-/de-icing system for aero-engine inlet guide vanes," *Appl. Therm. Eng.*, vol. 167, pp. 114778, Feb. 2020.
- [2] K. M. Al-Khalil and C. Horvath, *Validation of NASA Thermal Ice Protection Computer Codes Part 3: The Validation of Anti-ice*, NASA/TM-2001-210907, AIAA-97-0051, Glenn Research Center, Cleveland, OH, 2001.
- [3] P. E. Poinsatte and G. J. Van Fossen, *Convective Heat Transfer Measurements from a NACA 0012 Airfoil in Flight and in the NASA Lewis Icing Research Tunnel*, NASA/TM-102448, AIAA-90-0199, Lewis Research Center, Cleveland, 1990.
- [4] B. L. Messinger, "Equilibrium temperature of an unheated icing surface as a function of air speed," J. Aeronaut. Sci, vol. 20, no. 1, pp. 29-42, 1953.
- [5] X. Bu and G. Lin, "Numerical simulation of aircraft thermal anti-icing system based on a tight-coupling method," *Appl. Therm. Eng.*, vol. 169, 114778, 2020.
- [6] I. Langmuir and K. B. Blodgett, "*Mathematical investigation of water droplet trajectories*," Rep. RL-224, Gen. Elec. Res. Lab., Jan. 1945 (re-issued June 1949).